Turbo Packet Combining Strategies for the MIMO-ISI ARQ Channel

Tarik Ait-Idir, Member, IEEE, and Samir Saoudi, Member, IEEE

Abstract—This paper addresses the issue of efficient turbo packet combining techniques for coded transmission with a Chase-type automatic repeat request (ARQ) protocol operating over a multiple-input-multiple-output (MIMO) channel with intersymbol interference (ISI). First of all, we investigate the outage probability and the outage-based power loss of the MIMO-ISI ARQ channel when optimal maximum a posteriori (MAP) turbo packet combining is used at the receiver. We show that the ARQ delay (i.e., the maximum number of ARQ rounds) does not completely translate into a diversity gain. We then introduce two efficient turbo packet combining algorithms that are inspired by minimum mean square error (MMSE)-based turbo equalization techniques. Both schemes can be viewed as low-complexity versions of the optimal MAP turbo combiner. The first scheme is called signal-level turbo combining and performs packet combining and multiple transmission ISI cancellation jointly at the signal-level. The second scheme, called symbol-level turbo combining, allows ARQ rounds to be separately turbo equalized, while combining is performed at the filter output. We conduct a complexity analysis where we demonstrate that both algorithms have almost the same computational cost as the conventional log-likelihood ratio (LLR)-level combiner. Simulation results show that both proposed techniques outperform LLR-level combining, while for some representative MIMO configurations, signal-level combining has better ISI cancellation capability and achievable diversity order than that of symbol-level combining.

Index Terms—Automatic repeat request (ARQ) mechanisms, multiple-input—multiple-output (MIMO), intersymbol interference (ISI), outage probability, turbo equalization, minimum mean square error (MMSE).

I. Introduction

A. Research Motivation

H YBRID-AUTOMATIC repeat request (ARQ) protocols and multiple-input-multiple-output (MIMO) play a key role in the evolution of current wireless systems toward high data rate wireless broadband standards [1]. While MIMO techniques allow the space and time diversities of the multi-antenna channel to be translated into diversity and/or multiplexing gains [2], hybrid-ARQ mechanisms exploit the ARQ delay, i.e., the maximum number of ARQ transmission rounds,

Paper approved by A. Lozano, the Editor for Wireless Network Access and Performance of the IEEE Communications Society. Manuscript received July 7, 2008; revised May 27, 2009. This work was partly supported by Maroc Telecom under contract number 105 10005462.06/PI. This paper was presented in part at the IEEE Wireless Communications and Networking Conference, Las Vegas, NV, March-April 2008, and in part at the IEEE International Workshop on Signal Processing and Applications, Sharjah, UAE, March 2008.

T. Ait-Idir is with the Communication Systems Department, INPT, Madinat Al-Irfane, Rabat, Morocco. He is also with Institut Telecom / Telecom Bretegne/LabSticc, Brest, France (email: aitidir@ieee.org).

S. Saoudi is with Institut Telecom / Telecom Bretegne/LabSticc, Brest, France. He is also with Université Européenne de Bretagne.

to reduce the frame error rate (FER) and therefore increase the system throughput [3], [4].

In the last few years, special interest has been paid to the joint design of the transmission combiner (also referred to as "packet combiner") and the signal processor (detection and/or equalization) receiver. Combining schemes targeting a joint design approach were first proposed by Samra and Ding for single antenna systems operating over intersymbol interference (ISI) channels [5], [6], [7], [8], and are called transmission combining with integrated equalization (IEO). In particular, it was shown in [8] that, when concatenated with an outer code, IEQ performs better than the iterative combining scheme introduced by Doan and Narayanan [9]. In iterative combining, multiple copies of the same packet are independently interleaved and combining is performed by iterating between multiple equalizers before channel decoding. The IEQ concept was then extended to MIMO systems with flat fading to jointly perform co-antenna interference (CAI) cancellation and transmission combining [10], [11], [12]. In parallel, several other MIMO ARQ architectures exploiting the high degree of freedom in the design of the MIMO ARQ transmitter were proposed (e.g. [14], [16], [13], [15], [17], [18], [19], [20]). Turbo coded ARQ schemes with iterative minimum mean square error (MMSE) frequency domain equalization (FDE) for single carrier transmission over broadband channel were proposed for direct sequence code division multiple access (DS-CDMA) and MIMO systems in [21] and [22], [23], respectively.

Recently, in a seminal paper by El Gamal *et al.* [24], the diversity–multiplexing tradeoff ¹ of the MIMO ARQ flat fading channel was characterized, and was referred to as diversity–multiplexing–delay tradeoff. The authors proved that the ARQ delay presents an important source of diversity even when the channel is constant over ARQ transmission rounds, a scenario referred to as long-term static channel. In particular, it was shown that operating over such a channel with a large ARQ delay results in a flat diversity–multiplexing tradeoff. This means that one can achieve full diversity and multiplexing gains if large ARQ windows are allowed. The diversity–multiplexing–delay tradeoff was then investigated in the case of delay-sensitive services and block-fading MIMO channels in [29] and [30], respectively.

B. In this Paper

Motivated by the IEQ concept [8] and the results in [24], we investigate efficient IEQ-aided packet combining strategies for

¹A fundamental tool for the design of space-time coding/multiplexing architectures initially proposed by Zheng and Tse for flat fading [25], and later extended to frequency selective fading [26], [27], [28].

coded transmission with hybrid–ARQ operating over MIMO-ISI channels. Our main objective is to reduce the number of ARQ rounds required to correctly decode a data packet while keeping the receiver complexity (computational load and memory requirements) affordable. In our design, packet combining is performed at each ARQ round by exchanging soft information in an iterative (turbo) fashion between the *soft packet combiner* and the soft-input–soft-output (SISO) decoder. We refer to this combining family as "turbo packet combining".

We focus on space-time bit-interleaved coded modulation (ST-BICM) transmitter schemes with Chase-type ARQ, i.e., the data packet is entirely retransmitted. The choice of ST-BICM is motivated by the simplicity of this coding scheme, and the efficiency of its iterative decoding (ID) receiver in achieving high diversity and coding gains over block-fading MIMO-ISI channels [31], [32], [33], [34], [35], [36]. Our work is still valid for other space-time codes (STCs). Note that some practical systems employ hybrid-ARO with incremental redundancy (IR). In IR-type ARQ, retransmissions only carry portions of the data packet. It presents an efficient technique for increasing the system throughput while keeping the error performance acceptable. In this paper, we restrict our work to Chase-type ARQ. Turbo combining techniques for broadband MIMO transmission with IR-type ARQ are left for future investigations.

First of all, we derive the optimal maximum a posteriori (MAP) turbo packet combining algorithm ² that makes use of all diversities available in the MIMO-ISI ARQ channel to perform transmission combining. The turbo packet combining strategies we introduce in this paper can be seen as lowcomplexity sub-optimal techniques of the MAP combining algorithm. An important ingredient in MAP turbo combining is an analogy between multiple transmissions and antennas, and which consists of considering ARQ rounds as virtual receive antennas. This allows the ARQ delay, i.e., maximum number of ARQ rounds, to be translated into receive diversity. We then analyze the outage performance of the MIMO-ISI ARQ channel. This analysis allows us to know how the ARQ delay influences the outage probability of the MIMO ARQ system. It also serves as a theoretical foundation for the turbo packet combiners we propose in this paper. We also investigate the outage-based power loss due to multiple transmission rounds. This analysis establishes that in the outage region of interest (corresponding to an outage between 10^{-2} and 10^{-3}) the power loss due to ARQ is below 0.25dB.

The next step in our work corresponds to the derivation of two turbo packet combining strategies for the MIMO-ISI ARQ channel. Both techniques are inspired by the unconditional MMSE turbo equalization schemes of [34] and [37]. The first algorithm, named *signal-level* turbo packet combining, presents a low-complexity version of MAP turbo combining. It performs packet combining and equalization using signals from all transmission rounds. In contrast to what was initially stated in [38], we show that the computational complexity of

this scheme is less sensitive to the number of ARQ rounds. Moreover, we provide an optimized implementation where it is not necessary for the receiver to store all signal vectors and channel matrices. The second combining scheme, namely, symbol-level turbo combining, performs soft equalization separately for each round, and combines multiple transmissions at the level of filter outputs. It has the same computational complexity and fewer memory requirements compared with the first scheme. We also show that receiver requirements (computational complexity and memory) of both turbo combining schemes are almost similar to those of conventional loglikelihood ratio (LLR)-level combining, where extrinsic LLRs corresponding to multiple transmissions are simply added together before SISO decoding. Finally, we provide numerical simulations for some MIMO configurations demonstrating the superior performance of the proposed algorithms compared with LLR-level combining, and the significant gains they offer with respect to both the outage probability and the matched filter bound (MFB).

Throughout the paper, the following notation is used. Superscript $^{\top}$ denotes transpose, and H denotes Hermitian transpose. $\mathbb{E}\left[.\right]$ is the mathematical expectation of the argument (.). When \mathbf{X} is a square matrix, $\det\left(\mathbf{X}\right)$ denotes the determinant of \mathbf{X} . For each complex vector $\mathbf{x} \in \mathbb{C}^N$, $\operatorname{diag}\left\{\mathbf{x}\right\}$ is the $N \times N$ diagonal matrix whose diagonal entries are the elements of \mathbf{x} . \mathbf{I}_N is the $N \times N$ identity matrix, and $\mathbf{0}_{N \times Q}$ denotes an all zero $N \times Q$ matrix. \otimes is the Kronecker product, and $j = \sqrt{-1}$.

The following sections of the paper are organized as follows. In Section II, we provide a description of the MIMO ARQ system model and introduce some assumptions considered in this paper. In Section III, we derive the structure of the optimal MAP turbo combining scheme, and analyze the outage probability and the outage-based power loss of the considered MIMO ARQ system. Section IV details the structure of the proposed combining schemes and discusses complexity issues. Numerical results are provided in Section V. The paper is concluded in Section VI.

II. SYSTEM MODEL AND ASSUMPTIONS

We consider a multi-antenna link operating over a frequency selective fading channel and using an ARQ protocol at the upper layer. The transmitter and the receiver are equipped with N_T transmit and N_R receive antennas, respectively. The MIMO-ISI channel is composed of L taps (index l = $0, \cdots, L-1$). Each data stream is encoded with the aid of a ρ -rate channel encoder, interleaved using a semi-random interleaver Π , then modulated and space-time multiplexed over the N_T transmit antennas. This presents a ST-BICM coding scheme. The mapping function that relates each set of M coded and interleaved bits $b_{1,t,i}, \cdots, b_{M,t,i}$ to a symbol $s_{t,i}$ that belongs to the constellation set \mathcal{S} is denoted φ : $\{0,1\}^M \to \mathcal{S}$, where $t=1,\cdots,N_T$, and $i=0,\cdots,T-1$ are the transmit antenna and the channel use indices, respectively, and $M = \log_2 |\mathcal{S}|$. The $N_T \times T$ symbol matrix corresponding to the entire frame is denoted

$$\mathbf{S} \triangleq [\mathbf{s}_0, \cdots, \mathbf{s}_{T-1}] \in \mathcal{S}^{N_T \times T}, \tag{1}$$

$$\mathbf{s}_i \triangleq \left[\mathbf{s}_{1,i}, \cdots, s_{N_T,i}\right]^{\top} \in \mathcal{S}^{N_T}$$
 (2)

²In this paper, optimality refers to the exploitation of delay, space, time, and multipath diversities of the MIMO-ISI ARQ channel to combine multiple transmissions.

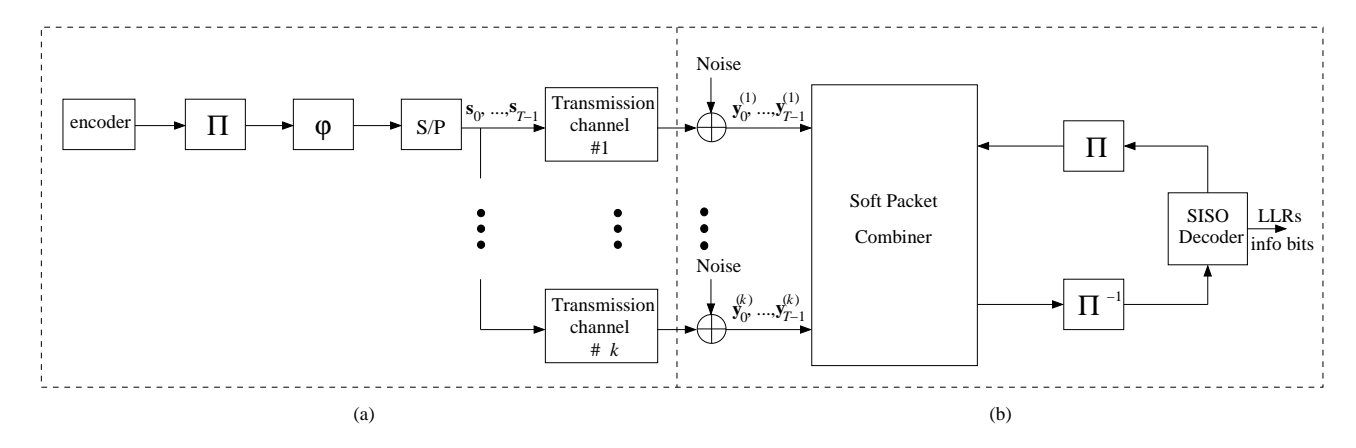


Figure 1. ST-BICM diagram with ARQ and turbo packet combining: (a) transmitter, (b) receiver

is the vector of transmitted symbols at time instant i. The rate of this transmission scheme is therefore $R = \rho M N_T$. When the transmitter receives a negative acknowledgment (NACK) message due to an erroneously decoded block, subsequent transmission rounds occur until the packet is correctly received or a preset maximum number of rounds, i.e., ARQ delay, K is reached. The round index is denoted $k = 1, \dots, K$. Reception of a positive acknowledgment (ACK) indicates a successful decoding and the transmitter moves on to the next block message. We suppose that the signaling channel carrying the one bit ACK/NACK feedback message is error free. In addition, we assume perfect packet error detection (typically, using a cyclic redundancy check (CRC) code). Therefore, a decoding failure corresponds to an erroneous decoding outcome after K rounds. We focus on Chase-type ARO mechanisms. i.e., the symbol matrix S is completely retransmitted. Both puncturing and mapping diversity, i.e., optimization of the mapping function over transmission rounds, are not investigated in this paper, and are left for future contributions. We use a zero padding (ZP) sequence $\mathbf{0}_{N_T \times L}$ to prevent interblock interference (IBI). The ST-BICM scheme with ARQ is depicted in Fig. 1. a. The MIMO-ISI channel is assumed to be quasi-static block fading, i.e., constant over a frame that spans T channel use and independently changes from round to round. This scenario corresponds to the so-called short-term static channel case where ARO transmission rounds see different and independent channel realizations [24]. The long-term static channel corresponds to the case where the channel is constant over all rounds related to the transmission of the same information block, i.e., $\mathbf{H}_{l}^{(k)} = \mathbf{H}_{l} \ \forall k \in \{1, \cdots, K\}$. Note that in orthogonal frequency division multiplexing (OFDM) broadband wireless systems, the ARQ channel is rather shortterm static because frequency hopping is used to mitigate ISI. While in time division multiplexing (TDM)-based systems, the channel dynamic can be either short or long-term static depending on the Doppler spread. In addition, we suppose that the channel profile, i.e., number of paths and power distribution, is identical for at least K consecutive rounds. This is a reasonable assumption for slowly timevarying wireless fading channels because the channel profile dynamic is mainly related to the shadowing effect. At the kth round, the channel impulse response is represented by the

 $N_R \times N_T$ complex matrices $\mathbf{H}_0^{(k)}, \cdots, \mathbf{H}_{L-1}^{(k)}$ corresponding respectively to taps $0, \ldots, L-1$, and whose entries are zero-mean circularly symmetric Gaussian $h_{r,t,l}^{(k)} \sim \mathcal{CN}\left(0,\sigma_l^2\right)$, where $h_{r,t,l}^{(k)}$ denotes the (r,t)th element of matrix $\mathbf{H}_l^{(k)}$. The total energy of taps $l=0,\cdots,L-1$ is normalized to one, i.e., $\sum_{l=0}^{L-1} \sigma_l^2 = 1$. Therefore, the channel energy per receive antenna $r=1,\cdots,N_R$ is

$$\sum_{l=0}^{L-1} \sum_{t=1}^{N_T} \mathbb{E}\left[\left| h_{r,t,l}^{(k)} \right|^2 \right] = N_T.$$
 (3)

We suppose that no channel knowledge is available at the transmitter. Equal power transmission turns out to be the best power allocation strategy. In addition, under the assumption of infinitely deep interleaving, and by normalizing the symbol energy to one, we get

$$\mathbb{E}\left[\mathbf{s}_{i}\mathbf{s}_{i}^{H}\right] = \mathbf{I}_{N_{T}}.\tag{4}$$

At the kth round, after down-conversion and sampling at the symbol rate, the baseband complex received signal on the rth antenna and at time instant i is

$$y_{r,i}^{(k)} = \sum_{l=0}^{L-1} \sum_{t=1}^{N_T} h_{r,t,l}^{(k)} s_{t,i-l} + n_{r,i}^{(k)},$$
 (5)

where $n_{r,i}^{(k)}$ is the noise on the rth antenna, and $\mathbf{n}_i^{(k)} \triangleq \left[n_{1,i}^{(k)}, \cdots, n_{N_R,i}^{(k)}\right]^{\top} \sim \mathcal{CN}\left(\mathbf{0}_{N_R \times 1}, \sigma^2 \mathbf{I}_{N_R}\right)$.

III. OPTIMAL TURBO PACKET COMBINING AND OUTAGE ANALYSIS

In this section, we provide a brief description of the structure of the turbo packet combining concept we propose in this paper, and introduce the optimal MAP turbo combiner. We also investigate the outage probability and the outage-based transmit power loss then provide a numerical analysis.

A. General Architecture and Optimal Turbo Combining

The turbo packet combining strategies we propose in this paper allow decoding of a data packet transmitted over multiple MIMO-ISI channels in an iterative (turbo) fashion through

$$\phi_{m,t,i,n}^{e} = \log \frac{\Pr\left\{\mathbf{y}^{(k)} \mid b_{m,t,i} = 1 ; \mathbf{H}_{0}^{(1)}, \cdots, \mathbf{H}_{L-1}^{(k)}, a \, priori \, \text{LLRs}\right\}}{\Pr\left\{\mathbf{y}^{(k)} \mid b_{m,t,i} = 0 ; \mathbf{H}_{0}^{(1)}, \cdots, \mathbf{H}_{L-1}^{(k)}, a \, priori \, \text{LLRs}\right\}},$$
(8)

$$\phi_{m,t,i,n}^{e} = \log \frac{\sum_{\mathbf{s} \in \mathcal{S}_{m,t,i}^{1}} \exp \left\{ -\frac{1}{2\sigma^{2}} \left\| \mathbf{y}^{(k)} - \mathbf{H}^{(k)} \mathbf{s} \right\|^{2} + \sum_{(m',t',i') \neq (m,t,i)} \varphi_{m'}^{-1} \left(x_{t',i'} \right) \phi_{m',t',i',n}^{a} \right\}}{\sum_{\mathbf{s} \in \mathcal{S}_{m,t,i}^{0}} \exp \left\{ -\frac{1}{2\sigma^{2}} \left\| \mathbf{y}^{(k)} - \mathbf{H}^{(k)} \mathbf{s} \right\|^{2} + \sum_{(m',t',i') \neq (m,t,i)} \varphi_{m'}^{-1} \left(x_{t',i'} \right) \phi_{m',t',i',n}^{a} \right\}},$$
(14)

the exchange of extrinsic information between the soft packet combiner and the SISO decoder. The main difference with conventional LLR-based packet combining is that multiple transmissions are combined before the computation of the soft information using a SISO packet combiner, while in LLR-level combining the soft outputs of different ARQ rounds are simply added together before channel decoding. The general block diagram is depicted in Fig. 1. b. Let N denote the number of turbo iterations performed between the combiner and the decoder at the kth round (index $n = 1, \dots, N$), and

$$\boldsymbol{\phi}_{t,i,n}^{e} \triangleq \left[\phi_{1,t,i,n}^{e}, \cdots, \phi_{M,t,i,n}^{e} \right]^{\top} \in \mathbb{R}^{M},$$

$$(t,i) \in \{1, \cdots, N_{T}\} \times \{0, \cdots, T-1\}$$
(6)

denote the vectors of extrinsic log-likelihood ratio (LLR) values generated by the soft combiner at iteration n. $\phi_{m,t,i,n}^e$ is the extrinsic information related to coded and interleaved bit $b_{m,t,i}$ at turbo iteration n. We similarly define a priori vectors

$$\boldsymbol{\phi}_{t,i,n}^{a} \triangleq \left[\phi_{1,t,i,n}^{a}, \cdots, \phi_{M,t,i,n}^{a}\right]^{\top} \in \mathbb{R}^{M},$$

available at the input of the soft combiner at iteration n. For the sake of notation simplicity, the round index is not used in LLRs. At the nth iteration of the kth round, the soft packet combiner makes use of the N_TT a priori vectors $\phi_{1,0,n}^a,\cdots,\phi_{N_T,T-1,n}^a$ and received signals to combine transmissions corresponding to rounds $1, \dots, k$, and compute extrinsic vectors $\phi_{1,0,n}^e$, \cdots , $\phi_{N_T,T-1,n}^e$. These extrinsic LLRs are de-interleaved and sent to the SISO decoder to compute a posteriori information about useful bits and extrinsic LLRs about coded bits. The generated extrinsic information is then interleaved and fed back to the soft combiner to serve as a priori information $\phi^a_{1,0,n+1},\cdots,\phi^a_{N_T,T-1,n+1}$ at next iteration n + 1. Note that the feedback of a NACK message does not necessarily mean that all information bits are erroneous. Therefore, extrinsic information generated by the SISO decoder during the last iteration of ARQ round k-1can be used as a priori information at the first iteration of ARQ round k. ³

Now, let us focus on the optimal soft packet combiner that allows the exploitation of all diversities, i.e., space, time, multipath, and retransmission, present in the MIMO-ISI ARQ channel to iteratively compute extrinsic information about coded and interleaved bits. First, let us introduce

$$\mathbf{y}_{i}^{(k)} \triangleq \left[y_{1,i}^{(k)} \cdots y_{N_{R},i}^{(k)} \right]^{\top} \tag{7}$$

that groups the signals received at time instant i of the kth round (5). We assume that the signals received at rounds $1, \dots, k$ (i.e., $\mathbf{y}_0^{(1)}, \dots, \mathbf{y}_{T-1}^{(k)}$) and their corresponding channel responses (i.e., $\mathbf{H}_0^{(1)}, \dots, \mathbf{H}_{L-1}^{(k)}$) are available at the receiver. Note that this assumption may present an important limiting factor (in addition to the computational complexity) for implementing the optimal turbo combiner, since all signals and channel responses have to be stored in the receiver. The low-complexity signal-level turbo combining strategy we introduce in Section IV relaxes this condition by using two recursions for keeping signals and channel matrices of previous rounds. At the nth iteration of round k, the optimal soft combiner computes extrinsic LLR about coded and interleaved bit $b_{m,t,i}$ according to the MAP criterion (8), where

$$\mathbf{y}^{(k)} \triangleq \left[\mathbf{y}_{T-1}^{(1)^{\mathsf{T}}}, \cdots, \mathbf{y}_{T-1}^{(k)^{\mathsf{T}}}, \cdots, \mathbf{y}_{0}^{(1)^{\mathsf{T}}}, \cdots, \mathbf{y}_{0}^{(k)^{\mathsf{T}}}\right]^{\mathsf{T}} \in \mathbb{C}^{kN_{R}T}.$$
(9)

Note that this vector representation is of a great importance because it allows us to view each transmission round as a source of an additional set of virtual N_R receive antennas. Therefore, ARQ diversity translates into space diversity (i.e., virtual receive antennas). The signal vector $\mathbf{y}^{(k)}$ corresponding to the transmission of matrix \mathbf{S} over k MIMO-ISI channels can be expressed as,

$$\mathbf{y}^{(k)} = \mathbf{H}^{(k)}\mathbf{s} + \mathbf{n}^{(k)},\tag{10}$$

where $\mathbf{H}^{(k)}$ is a $kN_RT \times N_TT$ block Toeplitz matrix,

 $^{^3}$ Generally speaking, iterative processing at round k will help correct information bits erroneously decoded during round k-1, while the LLR values of other bits remain the same.

$$\mathbf{H}^{(k)} \triangleq \begin{bmatrix} \mathbf{H}_{0}^{(1)} & & \mathbf{H}_{L-1}^{(1)} \\ \vdots & \cdots & \vdots \\ \mathbf{H}_{0}^{(k)} & & \mathbf{H}_{L-1}^{(k)} \\ & \ddots & & \ddots \\ & & \mathbf{H}_{0}^{(1)} & & \mathbf{H}_{L-1}^{(1)} \\ \vdots & \cdots & \vdots \\ \mathbf{H}_{0}^{(k)} & & \cdots & \vdots \\ \mathbf{H}_{0}^{(k)} & & & \mathbf{H}_{L-1}^{(k)} \end{bmatrix},$$
(11)

and

$$\mathbf{s} \triangleq \begin{bmatrix} \mathbf{s}_{T-1}^{\top}, \cdots, \mathbf{s}_{0}^{\top} \end{bmatrix}^{\top} \in \mathcal{S}^{N_{T}T}, \tag{12}$$

$$\mathbf{n}^{(k)} \triangleq \left[\mathbf{n}_{T-1}^{(1)^{\mathsf{T}}}, \cdots, \mathbf{n}_{T-1}^{(k)^{\mathsf{T}}}, \cdots, \mathbf{n}_{0}^{(1)^{\mathsf{T}}}, \cdots, \mathbf{n}_{0}^{(k)^{\mathsf{T}}}\right]^{\mathsf{T}} \in \mathbb{C}^{kN_{R}T}.$$
(13)

With respect to (10), extrinsic LLR given by (8) can now be expressed according to (14), where $\mathcal{S}_{m,t,i}^b = \{\mathbf{s} \in \mathcal{S}^{N_TT} \mid \varphi_m^{-1}(s_{t,i}) = b\}$, b = 0, 1.

B. Outage Probability and Outage-Based Transmit Power Loss

It is well known that for non-ergodic channels, i.e., block fading quasi-static channels, outage-probability P_{out} [39], [40], [41] is regarded as a meaningful tool for performance evaluation because it provides a lower bound on the block error rate (BLER) [42, p. 187]. The outage probability is defined as the probability that the mutual information, as a function of the channel realization and the average signal to noise ratio (SNR) γ per receive antenna, is below the transmission rate R. Mutual information rates of quasi-static frequency selective fading MIMO channel have been investigated in [43], [44].

1) Outage Probability: To derive the outage probability of the considered MIMO ARQ system, we use the renewal theory [45] which was first used by Zorzi and Rao to analyze the performance of ARQ protocols [46]. Recently, it was also used by [47], [24] to evaluate the performance of ARQ systems operating over wireless flat fading channels. Let \mathcal{A}_k denote the event that an ACK message is fed back at round k, and \mathcal{E}_k the event that the ARQ system is in outage at round k. Under the assumption of perfect packet error detection and error-free ACK/NACK feedback, and by applying the renewal theory, the outage probability for a given SNR γ and target rate R is given as

$$P_{out}^{R}(\gamma) = \Pr\left\{\mathcal{E}_{K}, \bar{\mathcal{A}}_{1}, \cdots, \bar{\mathcal{A}}_{K-1}\right\}. \tag{15}$$

Note that a Chase-type ARQ mechanism with an ARQ delay K can be viewed as a repetition coding scheme where K parallel sub-channels are used to transmit one symbol message [42, p. 194]. Therefore, (15) can be expressed as

$$P_{out}^{R}(\gamma) = \Pr\left\{\frac{1}{K}I\left(\mathbf{s}; \mathbf{y}^{(K)} \mid \mathbf{H}^{(K)}, \gamma\right) < R, \\ \bar{\mathcal{A}}_{1}, \cdots, \bar{\mathcal{A}}_{K-1}\right\}. \quad (16)$$

The virtual $KN_R \times N_T$ MIMO-ISI communication model at the Kth ARQ round is

$$\begin{bmatrix} \mathbf{y}_i^{(1)} \\ \vdots \\ \mathbf{y}_i^{(K)} \end{bmatrix} = \sum_{l=0}^{L-1} \begin{bmatrix} \mathbf{H}_l^{(1)} \\ \vdots \\ \mathbf{H}_l^{(K)} \end{bmatrix} \mathbf{s}_{i-l} + \begin{bmatrix} \mathbf{n}_i^{(1)} \\ \vdots \\ \mathbf{n}_i^{(K)} \end{bmatrix},$$

and the mutual information $I\left(\mathbf{s}; \mathbf{y}^{(K)} \mid \mathbf{H}^{(K)}, \gamma\right)$ in (16) can therefore be expressed in the case of i.i.d circularly symmetric complex Gaussian channel inputs as in [43], i.e.,

$$I\left(\mathbf{s}; \mathbf{y}^{(K)} \mid \mathbf{H}^{(K)}, \gamma\right) = \frac{1}{T} \sum_{i=0}^{T-1} \log_2\left(\det\left(\mathbf{I}_{KN_R} + \frac{\gamma}{N_T} \mathbf{\Lambda}_i^{(K)} \mathbf{\Lambda}_i^{(K)^H}\right)\right), \quad (17)$$

where $\Lambda_i^{(K)}$ is the discrete Fourrier transform (DFT) of the Kth round $KN_R \times N_T$ virtual MIMO-ISI channel at the ith frequency bin, i.e.,

$$\mathbf{\Lambda}_{i}^{(K)} = \sum_{l=0}^{L-1} \begin{bmatrix} \mathbf{H}_{l}^{(1)} \\ \vdots \\ \mathbf{H}_{l}^{(K)} \end{bmatrix} \exp\left\{-j\frac{2\pi}{T}il\right\}.$$
 (18)

2) Outage-Based Transmit Power Loss: To compare the outage probability performance of different ARQ configurations that operate at the same rate R but use different ARQ delays, we consider a short-term power constraint scenario where the same power Γ is used for all transmission rounds, i.e., the kth round transmit power is $\Gamma_k = \Gamma \ \forall k$. We evaluate the power loss incurred by multiple transmission rounds due to link outage. Note that system performance can be improved when a power control algorithm is jointly used with packet combining (typically, a long-term power constraint scenario), but this is beyond the scope of this paper. The average SNR present in the outage expression (16) is therefore given as

$$\gamma = \Gamma \frac{N_T}{\sigma^2}.\tag{19}$$

Let p count the number of information blocks, $q=1,\cdots,p$ denote the block index, and \mathcal{T}_q the number of rounds used for transmitting block q. Therefore, for a given ARQ delay K, average SNR γ , and rate R, the average transmit power is

$$\Gamma_{avg} = \lim_{p \to \infty} \frac{\sum_{q=1}^{p} \mathcal{T}_q}{p} \Gamma$$
$$= \mathbb{E} \left[\mathcal{T} \mid K, \gamma, R \right] \Gamma. \tag{20}$$

This indicates that an ARQ protocol with an ARQ delay K and operating with rate R at average SNR γ incurs an *outage-based transmit power loss* of $10\log_{10}\left(\mathbb{E}\left[\mathcal{T}\mid K,\gamma,R\right]\right)$ compared with an ARQ with K=1 round (i.e., no retransmissions).

C. Outage Analysis

In the following subsection we investigate, using simulations, both the outage probability and the outage-based transmit power loss for some MIMO-ISI ARQ configurations. This will serve as a theoretical foundation for the performance evaluation of turbo packet combiners which we will

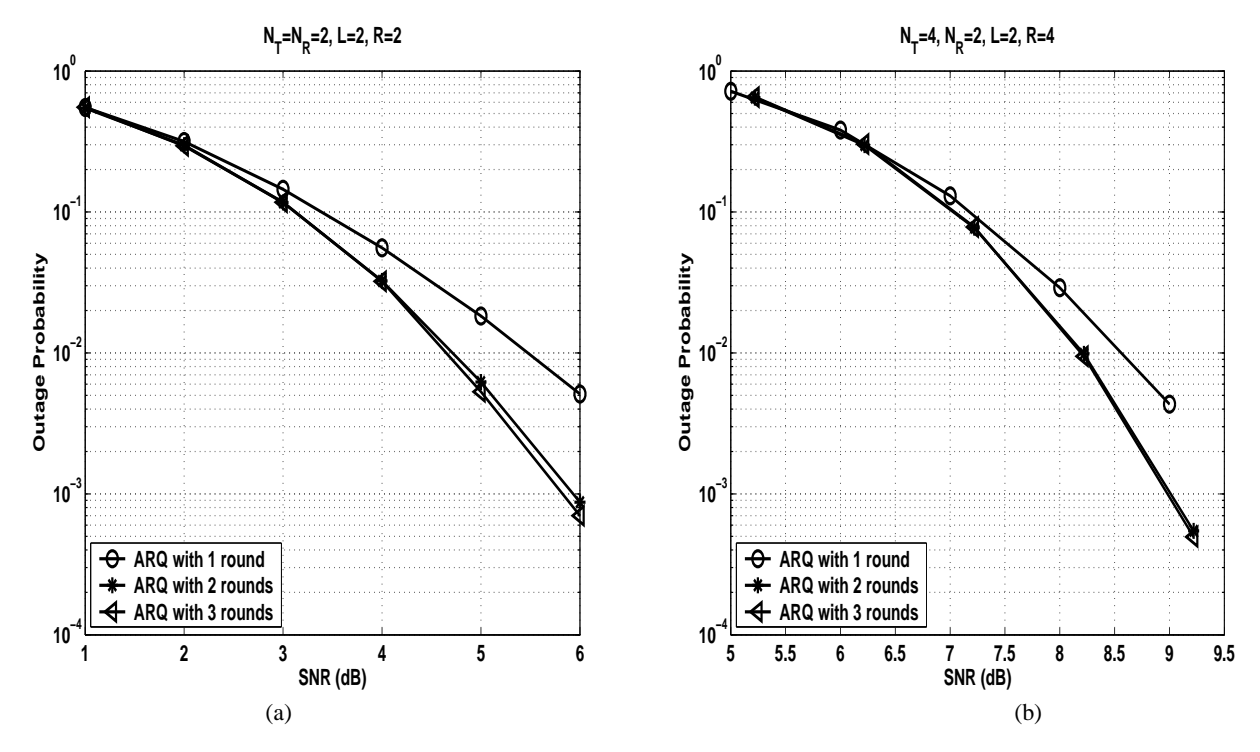


Figure 2. Outage probability versus the maximum number of rounds K for L=2 taps, $N_R=2$, and: (a) $N_T=2$, R=2, (b) $N_T=4$, R=4

introduce in the next subsection. Let us consider a MIMO-ISI channel with L=2 taps and equally distributed power, i.e., $\sigma_0^2=\sigma_1^2=\frac{1}{2}.$ We use Monte Carlo simulations to evaluate the outage probability (16) of the considered ARQ system. We choose T=256 channel use. At each round k, a $N_R \times N_T$ MIMO-ISI channel $\mathbf{H}_0^{(k)}$ and $\mathbf{H}_1^{(k)}$ is generated, and the mutual achievable rate after k rounds is computed using (17). If the target rate k is not reached and k is system moves on to the next round k+1. The ARQ process is stopped and another is started, either because of system outage (i.e., the achievable rate after k rounds is below k0 or non-outage (i.e., the achievable rate is greater than k1 after round k2 k).

In Fig. 2. a, we plot the outage probability as a function of the ARQ delay K for the two path MIMO-ISI channel with two transmit and two receive antennas $(N_T = N_R = 2)$, and a target rate R=2. The ARQ diversity gain, due to the short-term static channel dynamic, clearly appears when K=2. For instance, a gain of approximately 1dB is achieved at $5 * 10^{-3}$ outage compared with the case of K = 1 (i.e., no ARQ). When K=3, the outage probability performance is similar to that of K = 2. Fig. 2. b, shows the outage curves for $N_T=4$ and $N_R=2$ with a target rate R=4. We notice that as in the previous configuration, K=2 and K=3 have the same outage performance, while the overall diversity gain is more important than that corresponding to $N_T = N_R = 2$ (i.e., outage curve slopes are steeper than those of the first configuration). Note that the stacking procedure (9) relative to the optimal MAP-based turbo combiner creates kN_R virtual receive antennas after k rounds, but not all these virtual antennas will translate into a receive diversity, because the target rate R has to be maintained as it can be seen from the expression of the achievable information rate in (16). This justifies the outage performance saturation after K=2. This issue was recently addressed in [24] for MIMO ARQ with flat fading, and it was demonstrated that the diversity gain does not linearly increase with increase of the ARQ delay K. ⁴

In Fig. 3, we present the outage-based transmit power loss for the considered MIMO configurations. We observe that in the region of low SNR, the outage-based loss is significant for both K=2 and K=3. When the outage probability is below $<10^{-2}$ (the region corresponding to FER values typically required in practical systems), the transmit power loss is below 0.25dB. This indicates that in the corresponding SNR region, blocks are mainly error-free during the first transmission, and only a small number of frames require additional rounds.

Motivated by these theoretical results, in the next section we design a class of reduced complexity MMSE-based turbo combiners.

IV. Low Complexity MMSE-Based Turbo Packet Combining

It is obvious that the complexity of the MAP turbo combining technique presented in Subsection III-A is exponential in the number of transmit antennas and channel use. In this section, we introduce two low-complexity turbo packet combining techniques using the MMSE criterion, and analyze their computational cost and memory requirements.

 ^4In [24, Theorem 2], the authors demonstrated that for the case of a short-term static flat fading MIMO ARQ channel, the optimal diversity gain is $d^*\left(r_e,K\right)=Kf\left(\frac{r_e}{K}\right)~0\leq r_e<\min\left\{N_T,N_R\right\},$ where r_e is the multiplexing gain and f is the piecewise linear function connecting the points $(x,(N_T-x)\left(N_R-x\right))$ for $x=0,\ldots,\min\left\{N_T,N_R\right\}.$

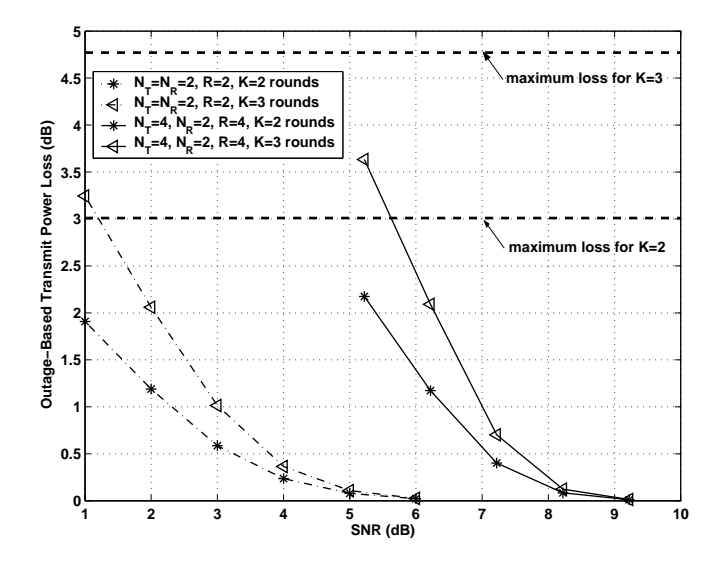


Figure 3. Outage-based transmit power loss for $N_T=N_R=2,\,R=2,$ and $N_T=4,\,N_R=2,\,R=4$

A. Signal-Level Turbo Combining

Let us recall the MAP turbo combiner block communication model (10) with a block length $\kappa=\kappa_1+\kappa_2+1\ll T$, where κ_1 and κ_2 are the lengths of the forward and backward filters, respectively. The corresponding $kN_R\kappa\times N_T\left(\kappa+L-1\right)$ sliding-window (around channel use i) communication model after k rounds is similar to (10), and is given as,

$$\underline{\underline{\mathbf{y}}}_{i}^{(k)} = \underline{\underline{\mathbf{H}}}^{(k)}\underline{\mathbf{s}}_{i} + \underline{\underline{\mathbf{n}}}_{i}^{(k)}, \tag{21}$$

where

$$\underline{\underline{\mathbf{y}}}_{i}^{(k)} \triangleq \left[\mathbf{y}_{i+\kappa_{1}}^{(1)^{\top}}, \cdots, \mathbf{y}_{i+\kappa_{1}}^{(k)^{\top}}, \cdots, \mathbf{y}_{i-\kappa_{2}}^{(1)^{\top}}, \cdots, \mathbf{y}_{i-\kappa_{2}}^{(k)^{\top}} \right]^{\top}$$
 (22)

$$\underline{\underline{\mathbf{n}}}_{i}^{(k)} \triangleq \left[\mathbf{n}_{i+\kappa_{1}}^{(1)^{\top}}, \dots, \mathbf{n}_{i+\kappa_{1}}^{(k)^{\top}}, \dots, \mathbf{n}_{i-\kappa_{2}}^{(1)^{\top}}, \dots, \mathbf{n}_{i-\kappa_{2}}^{(k)^{\top}}\right]^{\top}$$
(23)

are $kN_R\kappa \times 1$ complex vectors,

$$\underline{\mathbf{s}}_{i} \triangleq \left[\mathbf{s}_{i+\kappa_{1}}^{\top}, \cdots, \mathbf{s}_{i-\kappa_{2}-L+1}^{\top}\right]^{\top} \in \mathcal{S}^{N_{T}(\kappa+L-1)}, \tag{24}$$

and $\underline{\underline{\mathbf{H}}}^{(k)} \in \mathbb{C}^{kN_R\kappa \times N_T(\kappa + L - 1)}$ is defined similarly to (11).

To compute, at the nth iteration extrinsic information $\phi_{m,t,i,n}^e$ about bit $b_{m,t,i}$, using signals received during rounds $1,\cdots,k$, we jointly (over all rounds) cancel soft ISI in a parallel interference cancellation (PIC) fashion. This yields a soft ISI-free signal vector $\underline{\tilde{\mathbf{y}}}_{i|(t,n)}^{(k)} \in \mathbb{C}^{kN_R\kappa}$ expressed as,

$$\underline{\underline{\tilde{\mathbf{y}}}}_{i|(t,n)}^{(k)} \triangleq \underline{\underline{\mathbf{y}}}_{i}^{(k)} - \underline{\underline{\mathbf{H}}}^{(k)} \underline{\tilde{\mathbf{s}}}_{i|(t,n)}, \tag{25}$$

where $\underline{\tilde{\mathbf{s}}}_{i|(t,n)}$ is the conditional average of symbol vector $\underline{\mathbf{s}}_i$ with zero at the $(\kappa_1 N_T + t)$ th position,

$$\underline{\underline{\tilde{\mathbf{s}}}}_{i|(t,n)} \triangleq \mathbb{E}\left[\underline{\mathbf{s}}_{i} \mid \phi_{m',t',i',n}^{a} : (t',i') \neq (t,i)\right]. \tag{26}$$

The components of $\underline{\underline{\tilde{y}}}_{i|(t,n)}^{(k)}$ are then combined using an unconditional MMSE filter to produce the scalar input $\xi_{t,i,n}^{(k)}$ for the soft demapper. Applying the matrix inversion lemma [48] similarly to [37, eq. 6], we can write the output of the unconditional MMSE filter as,

$$\xi_{t,i,n}^{(k)} = \zeta_{t,n}^{(k)} \mathbf{e}_t^{\mathsf{T}} \underline{\underline{\mathbf{H}}}^{(k)^H} \mathbf{A}_n^{(k)^{-1}} \underline{\underline{\tilde{\mathbf{y}}}}_{i|(t,n)}^{(k)}, \tag{27}$$

where

$$\mathbf{A}_{n}^{(k)} = \underline{\underline{\mathbf{H}}}^{(k)} \Xi_{n} \underline{\underline{\mathbf{H}}}^{(k)^{H}} + \sigma^{2} \mathbf{I}_{k N_{R} \kappa} \in \mathbb{C}^{k N_{R} \kappa \times k N_{R} \kappa}, \quad (28)$$

$$\mathbf{\Xi}_n = \mathbf{I}_{\kappa+L-1} \otimes \tilde{\mathbf{\Xi}}_n \in \mathbb{C}^{N_T(\kappa+L-1) \times N_T(\kappa+L-1)}, \quad (29)$$

$$\tilde{\Xi}_n \triangleq \operatorname{diag}\left\{\tilde{\sigma}_{1,n}^2, \cdots, \tilde{\sigma}_{N_T,n}^2\right\},$$
 (30)

$$\mathbf{e}_{t} \triangleq \left[\underbrace{0, \cdots, 0}_{\kappa_{1} N_{T} + t - 1}, 1, \underbrace{0, \cdots, 0}_{(\kappa_{2} + L) N_{T} - t} \right]^{\top} \in \mathbb{C}^{N_{T}(\kappa + L - 1)}, \quad (31)$$

$$\zeta_{t,n}^{(k)} = \left(1 + \left(1 - \tilde{\sigma}_{t,n}^2\right) \mathbf{e}_t^{\mathsf{T}} \underline{\underline{\mathbf{H}}}^{(k)^H} \mathbf{A}_n^{(k)^{-1}} \underline{\underline{\mathbf{H}}}^{(k)} \mathbf{e}_t\right)^{-1}, \quad (32)$$

and $\tilde{\sigma}_{t,n}^2$ is the unconditional variance at iteration n of symbols $\{s_{t,i}\}_{i=0}^{T-1}$ transmitted over antenna t,

$$\tilde{\sigma}_{t,n}^{2} = \frac{1}{T} \sum_{i=0}^{T-1} \mathbb{E} \left[\left| s_{t,i} - \tilde{s}_{t,i,n} \right|^{2} \mid \phi_{m,t,i,n}^{a} : m = 1, \cdots, M \right],$$
(33)

$$\tilde{s}_{t,i,n} \triangleq \mathbb{E}\left[s_{t,i} \mid \phi_{m,t,i,n}^a : m = 1, \cdots, M\right]$$
 (34)

is the conditional average of symbol $s_{t,i}$ at iteration n.

Combining the soft PIC (25) and unconditional MMSE filtering (27) steps, and after some matrix manipulations, we can write the soft demapper input $\xi_{t,i,n}^{(k)}$ as,

$$\xi_{t,i,n}^{(k)} = \mathbf{F}_{t,n}^{(k)} \underline{\mathbf{z}}_{i}^{(k)} - \mathbf{B}_{t,n}^{(k)} \underline{\tilde{\mathbf{s}}}_{i|(t,n)}.$$
 (35)

 $\mathbf{F}_{t,n}^{(k)}$ and $\mathbf{B}_{t,n}^{(k)}$ are the forward and backward filters corresponding to antenna t at the nth iteration,

$$\mathbf{F}_{t,n}^{(k)} = \left(\sigma^2 + \left(1 - \tilde{\sigma}_{t,n}^2\right) \mathbf{e}_t^{\mathsf{T}} \mathbf{\Lambda}_n^{(k)} \mathbf{\Upsilon}^{(k)} \mathbf{e}_t\right)^{-1} \mathbf{e}_t^{\mathsf{T}} \mathbf{\Lambda}_n^{(k)}, \quad (36)$$

$$\mathbf{B}_{t,n}^{(k)} = \mathbf{F}_{t,n}^{(k)} \mathbf{\Upsilon}^{(k)}. \tag{37}$$

 ${f \Lambda}_n^{(k)},\, {f \underline{z}}_i^{(k)},$ and ${f \Upsilon}^{(k)}$ are given as

$$\mathbf{\Lambda}_n^{(k)} = \mathbf{I}_{N_T(\kappa + L - 1)} - \mathbf{\Upsilon}^{(k)} \left(\mathbf{\Upsilon}^{(k)} + \sigma^2 \mathbf{\Xi}_n^{-1} \right)^{-1}, \quad (38)$$

$$\begin{cases} \underline{\mathbf{z}}_{i}^{(k)} &= \underline{\mathbf{z}}_{i}^{(k-1)} + \underline{\mathbf{H}}^{(k)^{H}} \underline{\mathbf{y}}_{i}^{(k)} \\ \underline{\mathbf{z}}_{i}^{(0)} &= \mathbf{0}_{N_{T}(\kappa+L-1)\times 1}, \end{cases}$$
(39)

$$\begin{cases}
\boldsymbol{\Upsilon}^{(k)} &= \boldsymbol{\Upsilon}^{(k-1)} + \underline{\mathbf{H}}^{(k)^H} \underline{\mathbf{H}}^{(k)} \\
\boldsymbol{\Upsilon}^{(0)} &= \mathbf{0}_{N_T(\kappa+L-1)\times N_T(\kappa+L-1)}.
\end{cases} (40)$$

 $\underline{\mathbf{H}}^{(k)} \in \mathbb{C}^{N_R \kappa \times N_T(\kappa + L - 1)}$ and $\underline{\mathbf{y}}_i^{(k)}$ are the block Toeplitz matrix and signal output of the sliding-window communication model at round k, respectively, and are given as,

$$\phi_{m,t,i,n}^{e^{[Sig]}} = \log \frac{\sum_{s \in \mathcal{S}_{m}^{1}} \exp\left\{-\frac{1}{2\delta_{t,n}^{(k)^{2}}} \left| \xi_{t,i,n}^{(k)} - \alpha_{t,n}^{(k)} s \right|^{2} + \sum_{m' \neq m} \varphi_{m'}^{-1}(s) \phi_{m',t,i,n}^{a} \right\}}{\sum_{s \in \mathcal{S}_{m}^{0}} \exp\left\{-\frac{1}{2\delta_{t,n}^{(k)^{2}}} \left| \xi_{t,i,n}^{(k)} - \alpha_{t,n}^{(k)} s \right|^{2} + \sum_{m' \neq m} \varphi_{m'}^{-1}(s) \phi_{m',t,i,n}^{a} \right\}},$$
(45)

$$\phi_{m,t,i,n}^{e^{[Symb]}} = \log \frac{\sum_{s \in \mathcal{S}_{m}^{1}} \exp\left\{-\frac{1}{2} \left(\breve{\boldsymbol{\xi}}_{t,i,n}^{(k)} - s\breve{\boldsymbol{\alpha}}_{t,n}^{(k)}\right)^{H} \boldsymbol{\Delta}_{t,n}^{(k)^{-1}} \left(\breve{\boldsymbol{\xi}}_{t,i,n}^{(k)} - s\breve{\boldsymbol{\alpha}}_{t,n}^{(k)}\right) + \sum_{m' \neq m} \varphi_{m'}^{-1}(s) \phi_{m',t,i,n}^{a}\right\}}{\sum_{s \in \mathcal{S}_{m}^{0}} \exp\left\{-\frac{1}{2} \left(\breve{\boldsymbol{\xi}}_{t,i,n}^{(k)} - s\breve{\boldsymbol{\alpha}}_{t,n}^{(k)}\right)^{H} \boldsymbol{\Delta}_{t,n}^{(k)^{-1}} \left(\breve{\boldsymbol{\xi}}_{t,i,n}^{(k)} - s\breve{\boldsymbol{\alpha}}_{t,n}^{(k)}\right) + \sum_{m' \neq m} \varphi_{m'}^{-1}(s) \phi_{m',t,i,n}^{a}\right\}},$$
(47)

$$\underline{\mathbf{H}}^{(k)} \triangleq \begin{bmatrix} \mathbf{H}_0^{(k)} & \cdots & \mathbf{H}_{L-1}^{(k)} \\ & \ddots & & \ddots \\ & & \mathbf{H}_0^{(k)} & \cdots & \mathbf{H}_{L-1}^{(k)} \end{bmatrix}, \quad (41)$$

$$\underline{\mathbf{y}}_{i}^{(k)} \triangleq \left[\underline{\mathbf{y}}_{i+\kappa_{1}}^{(k)^{\top}}, \cdots, \underline{\mathbf{y}}_{i-\kappa_{2}}^{(k)^{\top}} \right]^{\top} \in \mathbb{C}^{N_{R}\kappa}, \tag{42}$$

$$\mathbf{y}_{\cdot}^{(k)} = \mathbf{\underline{H}}^{(k)} \mathbf{\underline{s}}_{i} + \mathbf{\underline{n}}_{i}^{(k)}, \tag{43}$$

$$\underline{\mathbf{n}}_{i}^{(k)} \triangleq \left[\mathbf{n}_{i+\kappa_{1}}^{(k)^{\top}}, \cdots, \mathbf{n}_{i-\kappa_{2}}^{(k)^{\top}}\right]^{\top} \in \mathbb{C}^{N_{R}\kappa}.$$
 (44)

Recursions (39) and (40) are easily obtained by invoking (22) and the general structure (11). Details about the derivation of (35) are omitted because of space limitation. Assuming the conditional soft demapper input is Gaussian, i.e., $\left(\xi_{t,i,n}^{(k)} \mid s_{t,i}\right) \sim \mathcal{N}\left(\alpha_{t,n}^{(k)}, \delta_{t,n}^{(k)^2}\right)$, extrinsic information $\phi_{m,t,i,n}^{e^{[Sig]}}$ can be computed according to (45), where

$$\begin{cases} \alpha_{t,n}^{(k)} &= \mathbf{B}_{t,n}^{(k)} \mathbf{e}_{t} \\ \delta_{t,n}^{(k)^{2}} &= \left(1 - \alpha_{t,n}^{(k)}\right) \alpha_{t,n}^{(k)}, \end{cases}$$
(46)

and $\mathcal{S}_m^b = \left\{ s \in \mathcal{S} \mid \varphi_m^{-1}(s) = b \right\}$. The signal-level combining algorithm is summarized in Table I.

Note that the forward-backward filtering structure (35) together with recursions (39) and (40) present the core part of the proposed algorithm, and allow a reduced computational complexity and an optimized implementation. Indeed, equations (39) and (40) allow to use at each ARQ round all signals and channel matrices corresponding to previous rounds $k-1,\cdots,1$ without being required to be explicitly stored in the receiver. This is performed in a recursive fashion using modified versions of the sliding window input and matrix (i.e., $\underline{\mathbf{H}}^{(k)^H}\underline{\mathbf{y}}_i^{(k)}$ and $\underline{\mathbf{H}}^{(k)^H}\underline{\mathbf{H}}^{(k)}$, respectively) at round k.

B. Symbol-Level Turbo Combining

In this combining scheme, we propose to perform equalization separately for each round k based on the communication model (43). Then, soft combining is conducted at the level of unconditional MMSE filter outputs: The output at iteration nof round k is combined with the outputs obtained at the last iteration of previous rounds $k-1, \dots, 1$. As in the previous

 $\underline{\mathbf{H}}^{(k)} \triangleq \begin{bmatrix} \mathbf{H}_{0}^{(k)} & \cdots & \mathbf{H}_{L-1}^{(k)} \\ & \ddots & & \ddots \\ & & \mathbf{H}_{0}^{(k)} & \cdots & \mathbf{H}_{L-1}^{(k)} \end{bmatrix}, \quad \text{(41)} \quad \text{subsection, let } \check{\xi}_{t,i,n}^{(k)} \text{ denote the filter output }^{5} \text{ at iteration } n \\ \text{of round } k, \text{ and } \left(\check{\xi}_{t,i,n}^{(k)} \mid s_{t,i}\right) \sim \mathcal{N}\left(\check{\alpha}_{t,n}^{(k)}, \check{\delta}_{t,n}^{(k)^{2}}\right). \text{ The soft demapper, which has a vector input in this case, computes extrinsic information } \phi_{m,t,i,n}^{e^{[Symb]}} \text{ according to (47), where}$

$$\boldsymbol{\xi}_{t,i,n}^{(k)} \triangleq \left[\boldsymbol{\xi}_{t,i,N}^{(1)}, \cdots, \boldsymbol{\xi}_{t,i,N}^{(k-1)}, \boldsymbol{\xi}_{t,i,n}^{(k)} \right]^{\top} \in \mathbb{C}^{k}, \tag{48}$$

$$\breve{\boldsymbol{\alpha}}_{t,n}^{(k)} \triangleq \left[\breve{\boldsymbol{\alpha}}_{t,N}^{(1)}, \cdots, \breve{\boldsymbol{\alpha}}_{t,N}^{(k-1)}, \breve{\boldsymbol{\alpha}}_{t,n}^{(k)}\right]^{\top} \in \mathbb{C}^{k}, \tag{49}$$

and $\pmb{\Delta}_{t,n}^{(k)}$ is the covariance matrix of $\left(m{ree}_{t,i,n}^{(k)}\mid s_{t,i}
ight)$ which can be approximated as (assuming residual ISI plus noise terms at different rounds are independent)

$$\Delta_{t,n}^{(k)} \approx \operatorname{diag} \left\{ \check{\delta}_{t,N}^{(1)^2}, \cdots, \check{\delta}_{t,N}^{(k-1)^2}, \check{\delta}_{t,n}^{(k)^2} \right\}.$$
(50)

The algorithm is summarized in Table II.

C. Complexity Analysis

In this subsection, we focus on the analysis of the computational cost of forward and backward filters as well as the memory requirements for the proposed algorithms. The other steps are similar and have the same complexity for both algorithms. We also provide comparisons with the conventional LLR-level combining technique.

In the case of signal-level turbo combining, the computation of forward and backward filters involves, at each round k and iteration n, one inversion of a $N_T(\kappa + L - 1) \times$ $N_T(\kappa + L - 1)$ matrix (i.e., matrix $\Upsilon^{(k)} + \sigma^2 \Xi_n^{-1}$ in eq. (38)) for computing $\Lambda_n^{(k)}$, and whose cost is $\mathcal{O}(N_T^3 \kappa^3)$ (assuming $\kappa \gg L$, and neglecting the cost of obtaining $\mathbf{\Xi}_n^{-1} = \mathbf{I}_{\kappa+L-1} \otimes \tilde{\mathbf{\Xi}}_n^{-1}$ since $\tilde{\mathbf{\Xi}}_n$ is diagonal). This indicates that the computational complexity of the signal-level combining scheme is less sensitive to k. The number of rounds only influences the number of additions required for obtaining vectors $\left\{\underline{\mathbf{z}}_i^{(k)}\right\}_{0\leq i\leq T-1}$ and matrix $\mathbf{\Upsilon}^{(k)}$, according to (39) and (40), respectively. The cost of these steps is

⁵The forward and backward filters can be easily derived using the equations in the previous subsection and assuming k = 1.

 $\label{thm:constraint} Table\ I$ Summary of the signal-level turbo packet combining algorithm

```
0. Initialization Initialize \Upsilon^{(0)} and \left\{\underline{\mathbf{z}}_{i}^{(0)}\right\}_{i=0}^{T-1} with \mathbf{0}_{N_{T}(\kappa+L-1)} and vectors \mathbf{0}_{N_{T}(\kappa+L-1)\times 1}, respectively.

1. Combining at round k
1.1. Update \left\{\underline{\mathbf{z}}_{i}^{(k)}\right\}_{i=0}^{T-1} and \Upsilon^{(k)} according to (39) and (40).

1.2. For n=1,\cdots,N
1.2.1. Compute: conditional symbol averages and unconditional variances using (34) and (33).

1.2.2. Compute: \Lambda_{n}^{(k)} using (38).
1.2.3. For t=1,\cdots,N_{T}
1.2.3.1. Compute: \mathbf{F}_{t,n}^{(k)}, \mathbf{B}_{t,n}^{(k)}, \alpha_{t,n}^{(k)} and \delta_{t,n}^{(k)} using (36), (37), and (46).
1.2.3.2. For each i=0,\cdots,T-1, compute the soft demapper input \xi_{t,i,n}^{(k)} according to (35).
1.2.3. For each m=1,\cdots,M, compute extrinsic information \phi_{m,t,i,n}^{e[Sig]} using (45).
1.2.4. End 1.2.3.
```

Table II SUMMARY OF THE SYMBOL-LEVEL TURBO PACKET COMBINING ALGORITHM

```
 \begin{array}{ll} \textbf{0.} & \textbf{Initialization} \\ & \textbf{Initialize} \left\{ \boldsymbol{\check{\xi}}_{t,i} \right\}_{i=0}^{T-1}, \ \boldsymbol{\check{\alpha}}_t, \ \text{and} \ \boldsymbol{\check{\delta}}_t^2 \ \text{with empty vectors for} \ t=1,\cdots,N_T. \\ \textbf{1.} & \textbf{Combining at round} \ k \\ \textbf{1.1.} & \textbf{For} \ n=1,\cdots,N \\ & \textbf{1.1.1.} & \textbf{Compute: conditional symbol averages and unconditional variances using (34) and (33).} \\ \textbf{1.1.2.} & \textbf{For} \ t=1,\cdots,N_T \\ & \textbf{1.1.2.1.} & \textbf{Compute: forward and backward filters,} \ \boldsymbol{\check{\alpha}}_{t,n}^{(k)}, \ \text{and} \ \boldsymbol{\check{\delta}}_{t,n}^{(k)}^2 \ \text{as in Subsection IV-A.} \\ \textbf{1.1.2.2.} & \textbf{For each} \ i=0,\cdots,T-1, \ \text{compute the filter output} \ \boldsymbol{\check{\xi}}_{t,i,n}^{(k)} \\ \textbf{1.1.2.3.} & \textbf{For each} \ m=1,\cdots,M, \ \text{compute extrinsic information} \ \boldsymbol{\phi}_{m,t,i,n}^{e[Symb]} \ \text{using (47).} \\ \textbf{1.2.3.} & \textbf{End 1.1.2.} \\ \textbf{1.2.4.} & \textbf{Ind 1.1.2.} \\ \textbf{1.2.5.} & \textbf{Ind 1.1.2.} \\ \textbf{1.2.6.} & \textbf{Ind 1.1.2.} \\ \textbf{1.2.7.} & \textbf{Ind 1.1.2.} \\ \textbf{1.2.7.} & \textbf{Ind 1.1.2.} \\ \textbf{1.2.8.} & \textbf{Ind 1.1.2.} \\ \textbf{1.2.9.} & \textbf{Ind 1.1.2.} \\ \textbf{1.
```

$$\Delta N_{Add} = N_T^2 \left(\kappa + L - 1\right)^2 + N_R \kappa T \tag{51}$$

for each round k>1. Note that the number of operations required for obtaining $\underline{\mathbf{H}}^{(k)^H}\underline{\mathbf{H}}^{(k)}$ and $\underline{\mathbf{H}}^{(k)^H}\underline{\mathbf{y}}_i^{(k)}$ in not considered in (51) since symbol-level combining also involves the same operations. Therefore, the computational cost of forward and backward filters is almost the same for both combining algorithms. Note that the significant reduction in the complexity of the signal-level combining scheme (with respect to the dimensionality of the sliding-window model (21) used by the algorithm) is due to recursion (40) which consists of writing $\underline{\underline{\mathbf{H}}}^{(k)^H}\underline{\underline{\mathbf{H}}}^{(k)}$ as the sum $\sum_{u=1}^k\underline{\underline{\mathbf{H}}}^{(u)^H}\underline{\underline{\mathbf{H}}}^{(u)}$.

Memory requirements for the two proposed schemes are determined by the update steps Tables I. **1.1** and II. **1.3**. For the signal-level combining technique, a $N_T (\kappa + L - 1) \times N_T (\kappa + L - 1)$ complex matrix is required to accumulate channel matrices $\underline{\mathbf{H}}^{(k)^H}\underline{\mathbf{H}}^{(k)}$ according to (40) (and therefore generating $\mathbf{\Upsilon}^{(k)}$), in addition to a $N_T (\kappa + L - 1) \times T$ complex matrix that serves to accumulate signal vectors $\left\{\underline{\mathbf{z}}_i^{(k)}\right\}_{i=0}^{T-1}$ using (39). Note that these two recursions, i.e., (39) and (40), avoid the storage of all signals and channel matrices as in MAP turbo combining. In the case of symbol-

level combining, only N_T complex matrices of size $K \times T$ and two $K \times N_T$ complex matrices are required to store filter outputs and their corresponding parameters, i.e., symbol gains and residual ISI plus thermal noise variances. Therefore, signal-level combining requires slightly more memory than its symbol-level counterpart, because only two or three ARQ rounds are considered (according to the outage analysis in Subsection III-C) and in general $\kappa \gg L$.

Finally, note that in the case of conventional LLR-level combining, soft equalization is separately performed for each ARQ round exactly as in symbol-level combining, while extrinsic LLRs are added together before decoding. This translates into N_TMTN real additions at each round, and a real vector of size N_TMT to combine extrinsic values. Therefore, the three combining strategies have similar implementation requirements. They slightly differ in the number of additions and storage memory.

V. NUMERICAL RESULTS

In this section, we provide simulated BLER and throughput performance for the proposed turbo packet combining techniques presented in Section IV. Considering some representative MIMO configurations, our main focus is to demonstrate that the signal-level turbo combining approach has better ISI cancellation capability and diversity gain than the symbol-level approach. We also show that both techniques provide better performance than conventional LLR-level combining.

A. Simulation Settings

In all simulations, we use an ST-BICM scheme composed of a 64-state $\frac{1}{2}$ -rate convolutional code with polynomial generators $(133_8, 171_8)$. The length of the code frame is 1800 bits including tail bits. We consider either quadrature phase shift keying (QPSK) or 16-state quadrature amplitude modulation (QAM) depending on the target rate R of the ST-BICM code. The MIMO-ISI channel has the same profile as in Subsection III-C, i.e., two equal power taps. With respect to the outage analysis in Section III, we consider a ARQ delay K=2. We verified, with simulations, that for the considered ST-BICM code, the improvement in BLER performance is only incremental when K > 2. Note that in [38], only a fourstate code is used, and performance results are reported with a maximum number of rounds K = 3. Simulations are carried out as in Subsection III-C, i.e., the transmission of an information block is stopped and the system moves on to the next block when an ACK message is received or the decoding outcome is erroneous after round K=2.

Note that the benefits of an ARQ mechanism appear in the region of low to moderate SNR, where multiple transmissions are required to help correct packets erroneously received after the first round. For high SNR values, ARQ may not be needed because most packets are correct after the first transmission. Therefore, we focus our analysis on the SNR region where BLER values, after the first round, are between 1 and 10^{-1} . In this region, an ARQ protocol is essential to have reliable communication. Our main goal is to analyze the ISI cancellation capability and the achieved diversity order for the proposed turbo combining schemes. We, therefore, evaluate the BLER performance per ARQ round. We also evaluate the throughput improvement offered by the proposed schemes. The SNR appearing in all figures is per symbol per receive antenna. For both schemes, we consider five turbo iterations for decoding an information block at each transmission. We compare the resulting performance with the outage probability and the MFB. Note that for the purpose of fair comparison, the computation of the outage performance does not take into account the rate distortion as in (16). The MFB curves are obtained for each transmission assuming perfect ISI cancellation and maximum ratio combining (MRC) of all time, space, multipath, and delay diversity branches.

B. Analysis

First we consider an ST-BICM code with $N_T=2$ and QPSK signaling. This corresponds to a rate R=2. The number of receive antennas is $N_R=2$, and the filter length is $\kappa=9$ ($\kappa_1=\kappa_2=4$) for all combiners. Fig. 4 compares the BLER performance for the signal-level, symbollevel, and LLR-level combining with the MFB and the outage probability. For both signal and symbol-level turbo combining, the performance improvement after the second ARQ round

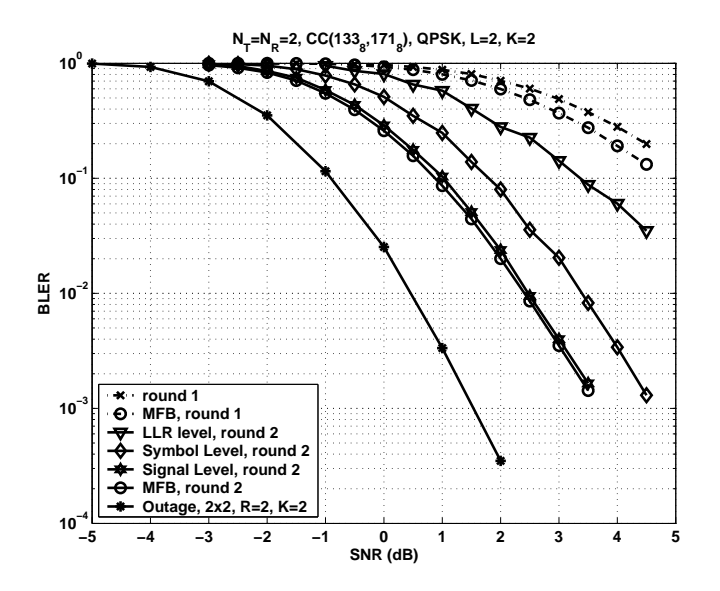
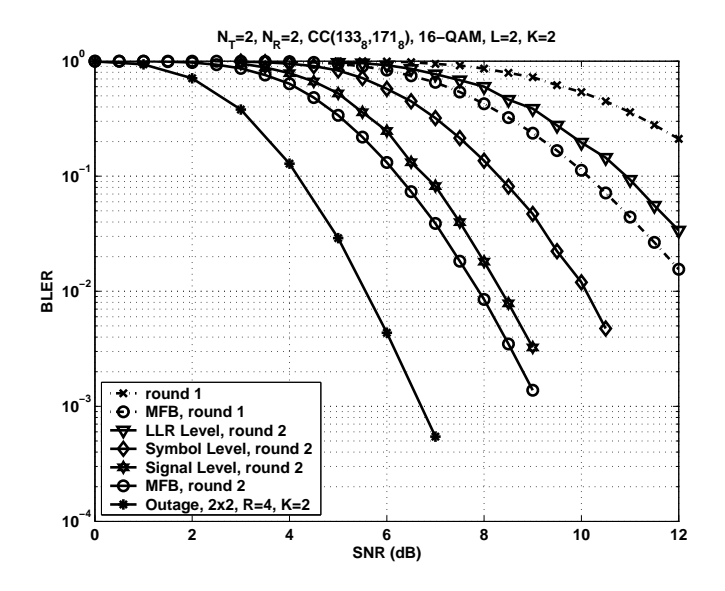
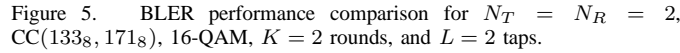


Figure 4. BLER performance comparison for $N_T=N_R=2$, $CC(133_8,171_8)$, QPSK, K=2 rounds, and L=2 taps.

is very significant compared with LLR-level combining. The signal-level combining scheme is shown to achieve the MFB while the symbol-level scheme presents approximately a gap of 1dB compared with the MFB. This means that signal-level combining has higher ISI cancellation capability than symbol-level combining. This result is due to the fact that in signal-level combining, each ARQ round is considered as a set of virtual N_R receive antennas. This allows the ARQ delay diversity to be efficiently exploited. On the other hand, both proposed schemes are shown to achieve the asymptotic slope of the outage probability.

Now, we turn to ST-BICM codes with rate R=4. Firstly, we consider a configuration similar to that of the previous case but using 16-OAM modulation. The filter length is kept equal to $\kappa = 9$. The BLER performance is reported in Fig. 5. In this scenario, the signal-level scheme clearly outperforms both the LLR-level and the symbol-level schemes. Indeed, the gap between the latter and the MFB is about 2.25dB. Both proposed techniques asymptotically achieve the diversity gain of the MIMO ARQ channel. In Fig. 6, we examine a ST-BICM code with $N_T = 4$, QPSK signaling, and $N_R = 2$. Note that this type of "unbalanced" configuration, i.e., more transmit than receive antennas, is suitable for the forward link. The filter length is increased to $\kappa = 13 \ (\kappa_1 = \kappa_2 = 6)$ for all schemes. The signal-level combining technique is shown to achieve BLER performance close to the MFB (the gap is less than 0.5dB), while both the LLR-level and the symbollevel techniques have a degraded probability of error (the gap between the symbol-level and the MFB is more than 3dB at $2 * 10^{-2}$ BLER). It is also important to note that signal-level combining manifests itself in almost achieving the diversity gain while it is shown that symbol-level combining fails to do so. This is mainly due to the fact that, at the second ARQ round, the signal-level scheme constructs a 4×4 virtual MIMO-ISI channel for ISI cancellation and symbol detection, while the MIMO configuration remains unbalanced in the





case of symbol-level combining. In Fig. 7, we compare the throughput performance of the three algorithm for the 4×2 configuration. It is shown that signal-level combining offers higher throughput. Also, note that while the MFB achieves the maximum throughput of 4bit/s/Hz, the proposed techniques saturate around 2bit/s/Hz because most of the packets received in the first ARQ round are erroneous.

Finally, note that in practical systems, channel estimation presents the bottle-neck that causes performance loss. In [38], we evaluated the BLER performance for a low-rate ST-BICM code (typically, $N_T = N_R = 2$, and R = 2) with imprecise channel estimates and using signal-level turbo packet combining. We have shown that when MMSE channel estimation is performed in a turbo fashion together with turbo packet combining (i.e., channel is iteratively re-estimated at each ARQ round using both pilot symbols and soft LLRs), the performance loss is less than 0.5dB when K=2, and does not exceed 1dB when the ARQ delay is increased to K=3. Also, we have shown that even for the case of short-term static dynamic, turbo channel estimation can offer attractive BLER performance without requiring the re-transmission of the pilot sequence since channel estimation in subsequent ARQ rounds can rely only on soft LLRs.

VI. CONCLUSION

In this paper, we considered the design of efficient turbo packet combining schemes for MIMO ARQ protocols operating over frequency selective channels. First of all, we derived the structure of the optimal MAP packet combiner that exploits all the diversities available in the MIMO-ISI ARQ channel to perform transmission combining. Inspired by [47], [24], we then investigated the outage probability and the outage-based power loss for Chase-type MIMO ARQ protocols operating over ISI channels. Then, we introduced two MMSE-based turbo combining schemes that exploit the delay diversity to perform transmission combining. The signal-level scheme considers an ARQ round as a set of virtual

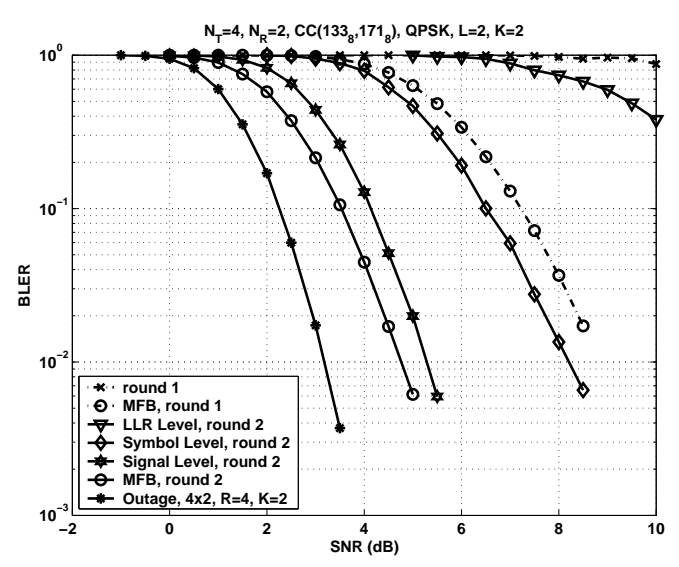


Figure 6. BLER performance comparison for $N_T=4$, $N_R=2$. $CC(133_8,171_8)$, QPSK, K=2 rounds, and L=2 taps.

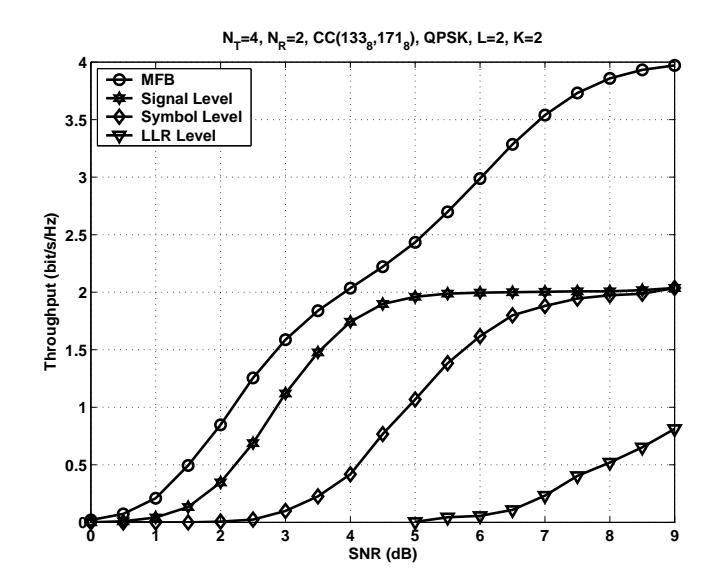


Figure 7. Throughput performance comparison for $N_T=4,\ N_R=2,\ {\rm CC}(133_8,171_8),\ {\rm QPSK},\ K=2$ rounds, and L=2 taps.

receive antennas and performs packet combining jointly with ISI cancellation. The symbol-level scheme separately equalizes multiple transmissions, while combining is performed at the level of filter outputs. We showed that both combining schemes have computational complexities similar to that of the conventional LLR-level combining. Finally, we presented simulation results that demonstrated that signal-level combining provides better BLER and throughput performance than that of symbol-level and LLR-level combining.

ACKNOWLEDGMENT

The authors would like to thank Prof. Tolga Duman for the comments he provided about an earlier version of this paper. They also would like to thank Prof. Angel Lozano for coordinating the review process, and the three anonymous reviewers for their very helpful comments and suggestions.

REFERENCES

- J. Peisa, S. Wager, M. Sagfors, J. Torsner, B. Goransson, T. Fulghum, C. Cozzo, and S. Grant, "High speed packet access evolution - concept and technologies," in Proc. 65th IEEE veh. tech. conf. VTC'07 Spring, Dublin, Ireland, Apr. 2007.
- [2] P. W. Wolniansky, G. J. Foschini, and R. A. Valenzuela, "V-BLAST: an architecture for realizing very high data rates over the rich scattering wireless channel," in Proc. Int. Symp. Signals, Systems, Electron., Pisa, Italy, Sep. 1998.
- [3] D. Chase, "Code combining-a maximum-likelihood decoding approach for combining an arbitrary number of noisy packets," *IEEE Trans. Commun.*, vol. COM-33, no. 5, pp. 385-393, May 1985.
- [4] B. Harvey, and S. Wicker, "Packet combining systems based on the Viterbi decoder," *IEEE Trans. Commun.*, vol. 42, no. 2-4, pp. 1544-1557, Feb.-Apr. 1994.
- [5] H. Samra, and Z. Ding, "Integrated iterative equalization for ARQ systems," in Proc. IEEE Int. Conf. on Acoustics, Speech, and Signal Processing (ICASSP), Orlando, FL, May 2002.
- [6] H. Samra, and Z. Ding, "Integrated iterative equalization for ARQ systems," in Proc. IEEE Int. Symp. on Info. Theory (ISIT), Lausanne, Switzerland, Jun., 2002.
- [7] H. Samra, and Z. Ding, "Precoded integrated equalization for packet retransmissions," in Proc. 36th IEEE Asilomar Conf. on Signals, Systems, and Computers, Monterey, CA, Nov., 2002.
- [8] H. Samra, and Z. Ding, "A hybrid ARQ protocol using integrated channel equalization," *IEEE Trans. Commun.*, vol. 53, no. 12, pp. 1996-2001, Dec. 2005.
- [9] D. N. Doan, and K. R. Narayanan, "Iterative packet combining schemes for intersymbol interference channels," *IEEE Trans. Commun.*, vol. 50, no. 4, pp. 560-570, Apr. 2002.
- [10] E. N. Onggosanusi, A. G. Dabak, Y. Hui, and G. Jeong, "Hybrid ARQ transmission and combining for MIMO systems," in Proc. IEEE Int. Conf. Commun., vol. 5, May 2003, pp. 3205-3209.
- [11] H. Samra, and Z. Ding, "Sphere decoding for retransmission diversity in MIMO flat-fading channels," in Proc. IEEE Int. Conf. on Acoustics, Speech, and Signal Processing (ICASSP), Montreal, Canada, May 2004.
- [12] H. Samra, and Z. Ding, "New MIMO ARQ protocols and joint detection via sphere decoding," *IEEE Trans. Sig. Proc.* vol. 54, no. 2, pp. 473-482, Feb. 2006.
- [13] H. Zheng, A. Lozano, and M. Haleem, "Multiple ARQ processes for MIMO systems," in Proc. 13th IEEE Intern. Symp. Personal Indoor and Mobile Radio Commun. (PIMRC), Lisbon, Portugal, Sep. 2002.
- [14] Zhihong Ding, and M. Rice, "Type-i hybrid-ARQ using MTCM spatio-temporal vector coding for MIMO systems," in Proc. IEEE Int. Conf. on Commun. (ICC), Anchorage, AK, May 2003.
- [15] A. Hottinen, and O. Tirkkonen, "Matrix modulation and adaptive retransmission," in Proc. 7th IEEE Intern. Symp. Sig. Proc. and Applications (ISSPA), Paris, France, Jul. 2003.
- [16] T. Koike, H. Murata, and S. Yoshida, "Hybrid ARQ scheme suitable for coded MIMO transmission," in Proc. IEEE Int. Conf. on Commun. (ICC), Paris, France, Jun. 2004.
- [17] S. Ibi, T. Matsumoto, S. Sampei, and N. Morinaga, "EXIT chart-aided adaptive coding for MMSE turbo equalization with multilevel BICM," *IEEE Commun. Lett.*, vol. 10, no. 6, pp. 486–488, Jun. 2006.
- [18] D. Krishnaswamy, and S. Kalluri, "Multi-level weighted combining of retransmitted vectors in wireless communications," in Proc. IEEE Veh. Technol. Conf., (VTC), Montreal, Canada, Sep. 2006.
- [19] E. W. Jang, J. Lee, H.-L. Lou, and J. M. Cioffi, "Optimal combining schemes for MIMO systems with hybrid ARQ," in Proc. IEEE Intern. Symp. Info. Theory (ISIT), Nice, France, Jun. 2007.
- [20] S. Ibi, T. Matsumoto, R. Thoma, S. Sampei, and N. Morinaga, "EXIT chart-aided adaptive coding for multilevel BICM with turbo equalization in frequency-selective MIMO channels," *IEEE Trans. Veh. Technol.*, vol. 56, no. 6, pp. 3757–3769, Nov. 2007.
- [21] D. Garg, and F. Adachi, "Packet access using DS-CDMA with frequency-domain equalization," *IEEE Journal Select. Areas in Com*mun., vol. 24, no. 1, Jan. 2006.
- [22] A. Nakajima, D. Garg, and F. Adachi, "Throughput of turbo coded hybrid ARQ using single-carrier MIMO multiplexing," in Proc. 61st IEEE veh. technol. conf. VTC'05 Spring, Stockholm, Sweden, 2005.
- [23] A. Nakajima, and F. Adachi, "Iterative joint PIC and 2D MMSE-FDE for turbo-coded HARQ with SC-MIMO multiplexing," in Proc. 63rd IEEE veh. technol. conf. VTC'06 Spring, pp. 2503-2507, Melbourne, Australia, May. 2006.

- [24] H. El Gamal, G. Caire, and M. O. Damen, "The MIMO ARQ channel: diversity-multiplexing-delay tradeoff," *IEEE Trans. Inf., Theory*, vol. 52, no. 8, Aug. 2006, pp. 3601-3621.
- [25] L. Zheng, and D. N. C. Tse, "Diversity and multiplexing: Afundamental tradeoff in multiple antenna channels," *IEEE Trans. Inf. Theory*, vol. 49, no. 5, pp. 1073–1096, May 2003.
- [26] A. Medles, and D. T. M. Slock, "Optimal diversity vs multiplexing tradeoff for frequency selective MIMO channels", in Proc Intern. Symp. Info. Theory (ISIT), Adelaide, Australia, Sept. 2005.
- [27] D. T. M. Slock, "On the diversity-multiplexing tradeoff for frequency-selective MIMO channels," in Proc. Info. Theory and App. (ITA) Workshop, San Diego, CA, Jan-Feb., 2007.
- [28] P. Coronel, and H. Bölcskei, "Diversity-multiplexing tradeoff in selective-fading MIMO channels," in Proc. Intern. Symp. Info. Theory (ISIT), Nice, France, Jun. 2007.
- [29] T. Holliday, A. Goldsmith, and H. V. Poor, "The impact of delay on the diversity, multiplexing, and ARQ tradeoff," in Proc. IEEE Int. Conf. on Commun. (ICC), Istanbul, Turkey, Jun. 2006.
- [30] A. Chuang, A. Guillen i Fabregas, L.K. Rasmussen, I.B. Collings, "Optimal throughput-diversity-delay tradeoff in MIMO ARQ block-fading channels," *IEEE Trans. Inf., Theory*, vol. 54, no. 9, Sep. 2008, pp. 3968-3986.
- [31] S. L. Ariyavisitakul, "Turbo space-time processing to improve wireless channel capacity," in Proc. IEEE Commun. Conf., vol. 3, pp. 1238-1242, Jun. 2000.
- [32] A. M. Tonello, "MIMO MAP equalization and turbo decoding in interleaved space time coded systems", *IEEE Trans. Commun.*, vol. 51, no. 2, pp. 155-160, Feb. 2003.
- [33] R. Visoz, and A. O. Berthet, "Iterative decoding and channel estimation for space-time BICM over MIMO block fading multipath AWGN channel", *IEEE Trans. Commun.*, vol. 51, no. 8, pp. 1358-1367, Aug. 2003
- [34] X. Wautelet, A. Dejonghe, and L. Vandendorpe, "MMSE-based fractional turbo receiver for space-time BICM over frequency selective MIMO fading channels," *IEEE Trans. Sig. Proc.*, vol. SIG-52, pp. 1804-1809, Jun. 2004.
- [35] R. Visoz, A. O. Berthet, and S.Chtourou, "A new class of iterative equalizers for space-time BICM over MIMO block fading multipath AWGN channel," *IEEE Trans. Commun.*, vol. 53, no. 12, pp. 2076-2091, Dec. 2005.
- [36] T. Ait-Idir, S. Saoudi, and N. Naja, "Space-time turbo equalization with successive interference cancellation for frequency selective MIMO channels," *IEEE Trans. Veh. Technol.*, vol. 57, no. 5, pp. 2766-2778, Sep. 2008.
- [37] M. Tüchler, A. C. Singer, and R. Koetter, "Minimum mean squared error equalization using *a priori* information," *IEEE Trans. Sig. Proc*, vol. 50, no. 3, pp. 673–683, Mar. 2002.
- [38] T. Ait-Idir, H. Chafnaji, and S. Saoudi, "Joint hybrid ARQ and Iterative Space-Time Equalization for Coded Transmission over the MIMO-ISI Channel," in Proc. IEEE Wireless Commun. Net. Conf. (WCNC), Las Vegas, NV, Mar-Apr. 2008.
- [39] L. H. Ozarow, S. Shamai, and A. D. Wyner, "Information theoretic considerations for cellular mobile radio," *IEEE Trans. Inform. Theory*, vol. 43, pp. 359–378, May 1994.
- [40] I. E. Telatar, "Capacity of multi-antenna Gaussian channels," Europ. Trans. Telecommun., vol. 10, no. 6, pp. 585–595, Nov./Dec.1999.
- [41] G. J. Foschini and M. J. Gans, "On limits of wireless communications in a fading environment when using multiple antennas," Wireless Personal Commun., vol. 6, pp. 311–335, Mar. 1998.
- [42] D. Tse, and P. Viswanath, "Fundamentals of Wireless Communication," Cambridge University Press, May 2005.
- [43] H. El Gamal, A. R. Hammons, Y. Liu, M. P. Fitz, and O. Y. Takeshita, "On the design of space-time and space-frequency codes for MIMO frequency-selective fading channels," *IEEE Trans. Inform. Theory*, vol. 49, no 9, pp. 2277–2292, Sep. 2003.
- [44] Z. Zhang, T. M. Duman, and E. M. Kurtas, "Achievable information rates and coding for MIMO systems over ISI channels and frequencyselective fading channels," *IEEE Trans. Commun.*, vol. 52, no 10, pp. 1698–1710, Oct. 2004.
- [45] R. Wolff, Stochastic Modeling and the Theory of Queues. Upper Saddle River, NJ: Prentice-Hall, 1989.
- [46] M. Zorzi, and R. R. Rao, "On the use of renewal theory in the analysis of ARQ protocols," *IEEE Trans. Commun.*, vol. 44, pp. 1077–1081, Sept. 1996.
- [47] G. Caire, and D. Tuninetti, "ARQ protocols for the Gaussian collision channel," *IEEE Trans. Inf. Theory*, vol. 47, no. 4, pp. 1971–1988, Jul. 2001

[48] S. Haykin, Adaptive Filter Theory, 3rd Ed. Upper Saddle River, NJ: Prentice-Hall, 1996.



Tarik Ait-Idir (S'06–M'07) was born in Rabat, Morocco, in 1978. He received the "diplôme d'ingénieur d'état" in telecommunications from INPT, Rabat, and the Ph.D. degree in electrical engineering from ENST Bretagne, Brest, France, in 2001, and 2006, respectively.

He is currently an Assistant Professor of wireless communications at the Communication Systems department, INPT, Rabat. He is also an adjunct researcher with Institut Telecom / Telecom Bretegne/LabSticc. From July 2001 to February

2003 he was with Ericsson. His research interests include PHY and crosslayer aspects of MIMO systems, relay communications, and dynamic spectrum management.

Dr. Ait-Idir has been on the technical program committee of several IEEE conferences, including ICC, WCNC, PIMRC, and VTC, and chaired some of their sessions. He has been a technical co-chair of the MIMO Systems Symposium at IWCMC 2009.



Samir Saoudi (M'01) was born in Rabat, Morocco, on November 28, 1963. He received the "diplôme d'ingénieur d'état" from ENST Bretagne, Brest, France, in 1987, the Ph.D. degree in telecommunications from the 'Université de Rennes-I' in 1990, and the "Habilitation à Diriger des Recherches en Sciences" in 1997.

Since 1991, he has been with the Signal and Communications department, Institut Telecom / Telecom Bretegne/LabSticc, where he is currently a Professor. He is also with Université Européenne de Bretagne.

In summer 2009, he has visited Orange Labs-Tokyo. His research interests include speech and audio coding, non parametric probability density function estimation, CDMA techniques, multiuser detection and MIMO techniques for UMTS and HSPA applications. His teaching interests are signal processing, probability, stochastic processes and speech processing.

Dr. Saoudi supervised more than 20 Ph.D. Students. He is the author and/or coauthor of around eighty publications. He has been the general chairman of the second International Symposium on Image/Video Communications over fixed and mobile networks (ISIVC'04).